Glass Transition Behaviors of a Polyurethane Hard Segment based on 4,4′-Diisocyanatodiphenylmethane and 1,4-Butanediol and the Calculation of Microdomain Composition

Teng Ko Chen,* Jia Yeong Chui, and Tien Shou Shieh

Department of Chemical Engineering, National Central University, Chung-Li 32054, Taiwan, Republic of China

Received December 18, 1996; Revised Manuscript Received April 29, 1997[⊗]

ABSTRACT: The long-term confusing glass transition temperature, T_g, and specific heat capacity, ΔC_p, of the 4,4′-diisocyanatodiphenylmethane (MDI) and 1,4-butanediol (BD) hard segment in segment polyurethanes have been clearly evidenced by using a new series of completely phase-mixed polyurethanes while being extrapolated to 100% hard segment content. The hard segment T_g and ΔC_p thus obtained are 108 °C and 0.38 J/g °C, respectively, which are equivalent to the reported Tg and ΔC_p of a high molecular weight MDI−BD homopolymer. In addition, if a single homogeneous phase is present, the observed ΔC_p and T_g are found to be given by the linear weighted combination of the pure constituent values. This provides a simple relationship to access the composition of the individual microdomain in segment polyurethanes, providing that the phase-separate morphology does not affect the microdomain glass transition behavior.

Introduction

Segmented polyurethane elastomers are linear block copolymers of $-(HS)_n-$ type (H, hard segment; S, soft segment) whose versatile physical properties are generally attributed to their microphase-separation structure. The microphase-separation structures arises due to the incompatibility of the hard segment and the soft segment. However, most investigations have evidenced that the microphase separation is not complete.[1] Since the degree of microphase separation and microphase composition dominantly control polyurethane's physical properties, many investigators[1−8] paid much attention to the methods of characterizing the degree of microphase separation and microphase composition. Differential scanning calorimetry (DSC) is a most attractive tool for this purpose since measurement of the glass transition temperature, T_g, and the change of heat capacity, ΔC_p, at T_g are both quantitative and relatively easy, and based on the T_g and ΔC_p of the pure hard segment and pure soft segment, many theoretical[9−12] and semiempirical[5−7] relationships can be used for calculating the degree of microphase separation and the microphase composition. However, for the most important 4,4′-diisocyanatodiphenylmethane−1,4-butanediol (MDI−BD)-based polyurethane, DSC cannot identify the glass transition behaviors of the hard-segment-rich phase[13,14] due to formation of crystalline or ordered structures in the hard microdomain. These analytic methods were hampered by the lack of reliable values of hard segment's T_g, T_{gH°, and ΔC_p, ΔC_{pH°, as standards. Many controversies and inconclusive results have appeared in the literatures.[5,6,15,16] The following is a brief review of some of the previous endeavors for pursuing T_{gH° and ΔC_{pH°.

Owing to the glass transition temperature of a high molecular weight MDI−BD homopolymer is 110 °C[17] and the heat capacity of the MDI−BD hard segment in polyurethane is generally very small or almost undetectable. Camberlin and Pascault[5] proposed that the MDI−BD hard segment, while dissolved in the soft microphase, has the same effect as the MDI−BD homopolymer (T_g = 110 °C) to the microphase's T_g and has negligible contribution to the change in heat capacity at the microphase's glass transition temperature. However, these assumptions are inconsistent with their use of Fox's equation to model the composition of the soft microphase, since Couchman et al.,[10−12] from a classical thermodynamic viewpoint, have suggested that Fox's equation is based on the assumption that the heat capacities of both segments shall be equivalent. Unfortunately, many researchers followed these simple assumptions for their works.

Koberstein et al.[7] carried out DSC quench-mixing experiments to obtain T_g's and ΔC_p's from a series of segment polyurethanes in a homogeneous mixed state. On the basis of these data, they obtained the hard segment T_g from a linear least square fit of a generalized Fox equation[18] and the hard segment ΔC_p from a fit of linear weighted combinations of the pure constituent ΔC_p values. Although their results, T_{gH° = 109 °C and ΔC_{pH° = 0 J/g, agree with those suggested by Camberline and Pascult, the discrepancy with Couchman's argument had not been resolved. Koberstein[7] explained this discrepancy by the possible occurrence of a small amount of phase separation during quenching, which would have the effect of lowing the measured ΔC_p.

Recently, Koberstein et al.[15] used DSC and small angle X-ray scattering (SAXS) to study polyurethanes' microphase composition. On the basis of the above hard segment T_g and ΔC_p values and the literature-reported soft segment T_g, T_{gS° and ΔC_p, ΔC_{pS°, they first calculated microphase compositions by using a generalized Fox equation. Thereafter, they applied these calculated microphase compositions to calculate the hard (hard-segment-rich) microdomains' T_g and the polyurethanes' electron density variance. However, these later calculated T_g's were not consistent with the DSC hard microdomain T_g's which were assumed, after being thoroughly studied in conjunction with thermal mechanical analysis, to be the endothermic peaks appearing at 50−90 °C in their DSC thermogram.[15,19] On the other hand, the calculated electron density variances also did not agree with the experimental electron density variances from SAXS. In addition, they also

* Author to whom correspondence should be addressed.
[⊗] Abstract published in *Advance ACS Abstracts,* July 15, 1997.

S0024-9297(96)01863-3 CCC: $14.00

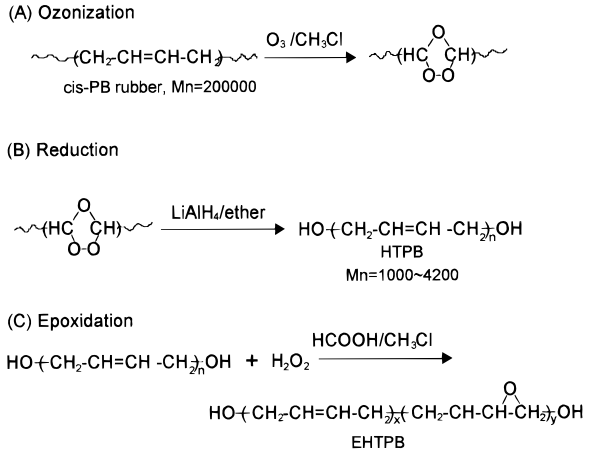

Figure 1. The reaction steps for the synthesis of EHTPB.

developed a method,[15] on the basis of the Couchman theory and SAXS analysis, to calculate $\Delta C_{p_{H^\circ}}$ while fixing $T_{g_{H^\circ}} = 109$ °C as standard. However, the value of $\Delta C_{p_{H^\circ}}$ ranged from 0.55 to 21 J/g °C as the hard segment contents ranged within 30%−70%. They explained that the self-contradictories were due to a number of reasons, i.e., the $T_{g_{H^\circ}}$ may be a function of its own molecular weight; the hard domain exhibited a crystalline structure; or the polyurethane may be a three-phase system, including the soft microphase, the hard amorphous phase, and the hard crystalline phase, and so on.

More recently, instead of using $\Delta C_{p_{H^\circ}} = 0$ J/g °C for studying the effect of annealing temperature on the microphase composition, Koberstein[20] applied a $\Delta C_{p_{H^\circ}} = 0.3$ J/g °C, which was calculated by the Simha-Boyer rule[21] ($T_g \Delta C_p = 27.5$ J/g). However, they did not explain why they had made this change.

From the above reviews, it is realized that a complete description of microdomain structure from DSC measurements is still hampered by the lack of the reliable hard segment T_g and ΔC_p values. To solve this problem, our strategies are to study the MDI−BD-based polyurethanes from two extremes, one with a series of complete phase-mixed polyurethanes and the other with a series of complete phase-separate polyurethanes. At these two extremes, the polyurethanes would provide very simplified structures, from which some basic, unambiguous structure-property relationships may be drawn. In this study, we present an experimental method to access the reliable hard segment T_{g_H} and ΔC_{p_H} values from a series of complete phase-mixed polyurethanes. This method employs a newly developed soft segment diol, epoxidized hydroxyl-terminated polybutadiene (EHTPB), to form a new series of polyurethanes (EHTPB-based PUs). As the epoxide content on the EHTPB increases or the molecular weight of the EHTPB decreases, we can achieve a "true" homogeneous phase with complete mixing of the hard and soft segments. The exhibited single glass transition when extrapolating to 100% hard segment content would give a set of the reliable T_g and ΔC_p values for the pure hard segments. Following this, we also discuss the methods to calculate polyurethane's microphase composition and the degree of phase separation.

Experimental Section

Materials. Figure 1 outlines the synthetic route to the epoxidized hydroxyl-terminated *cis*-polybutadiene (EHTPB), including ozonization, reduction, and epoxidation. The processes of ozonization and reduction first produced an hydroxyl-terminated polybutadiene (HTPB). The HTPBs used in this study were characterized to have 96% *cis*-butadiene structure, number average molecular weights ranging from 1000 to 4200, and both molecular weight distribution and average hydroxyl functionality equal to 2. The FTIR spectra of an HTPB and its parent high molecular weight *cis*-PB are given in Figure 2. The HTPB spectrum shows an additional broad hydroxyl group absorption at 3300 cm^{-1}. The complete chemical details were presented elsewhere.[22] These well-defined HTPBs were finally epoxidized to produce the EHTPBs. The yields of EHTPBs all exceed 97%. The ring-open reaction[23] did not occur during epoxidation as had been confirmed by FTIR and NMR analyses. The extent of epoxidation in HTPB was defined by the value of weight per epoxide (WPE), which can be determined by a titration method[31] or by a high-resolution NMR analysis. A high-resolution NMR spectrum and the method to calculate WPE are given in Figure 3. The complete chemical details for the epoxidation were also presented elsewhere.[23] Many EHTPBs had been synthesized; however, only a few were found useful for the present study. Table 1 lists the characteristics of the EHTPBs used in this study.

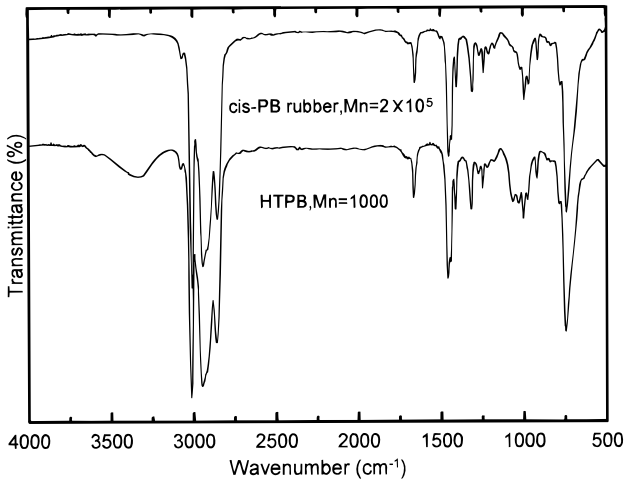

Figure 2. The FTIR spectra of a HTPB and its parent high molecular weight *cis*-PB rubber.

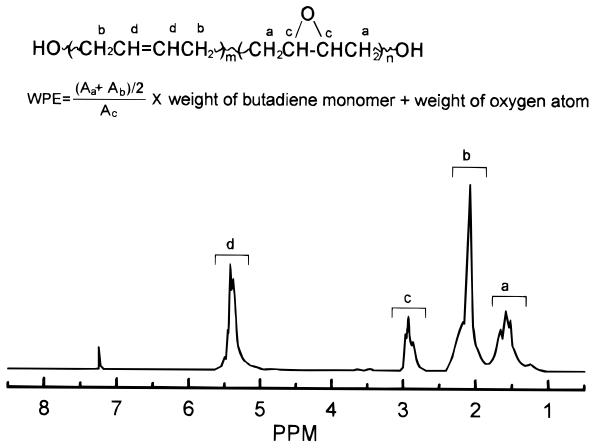

Figure 3. The NMR spectrum of an EHTPB prepolymer.

The EHTPBs were thoroughly degassed at 60 °C for 1 day before use. 4,4′-Diisocyanatodiphenylmethane (MDI; T.C.I. Co.) and chain extender 1,4-butanediol (BD; Aldrich) were used as received. Tetrahydrofuran (THF; Aldrich) and *N*,*N*′-dimethylacetamide (DMAc; Aldrich) were dried over molecular sieves before use.

1. Synthesis of Epoxidized Polybutadiene-Based Polyurethanes. The epoxidized polybutadiene-based polyurethanes (EHTPB-based PUs) were prepared in a mixed solvent system of THF to DMAc at 1:1 (v/v). The EHTPB solution, containing 0.15% stannous octotate as the catalyst, was added

Table 1. The Characteristics of Epoxidized Hydroxy-Terminated Polybutadiene

sample[a]	M_n before epoxidation[b]	WPE[c]	MWD (approx)	F_n (approx)
EHTPB-1000(360)	1000	360	2.0	2.0
EHTPB-1000(200)	1000	200	2.0	2.0
EHTPB-1650(210)	1650	210	2.0	2.0
EHTPB-2300(200)	2300	200	2.0	2.0
EHTPB-4200(210)	4200	210	2.0	2.0

[a] Samples are designated as EHTPB-*xxxx*(*yyy*) where *xxxx* denotes the number average molecular weight of EHTPB's precursor, HTPB, and *yyy* denotes the condition of epoxidation, WPE. [b] M_n is determined by vapor pressure osmometry in benzene solution at 45 °C. [c] WPE is determined by the method of Ray.[31]

Table 2. The Composition and Property of EHTPB-Based Polyurethanes

PU sample	soft segment type	hard segment content (%)	M_{nh}[a]	intrinsic viscosity η_{int} (dL/g)
PU-1000(360)-35	EHTPB-1000(360)	35	570	0.29
PU-1000(200)-28	EHTPB-1000(200)	28	420	0.36
PU-1000(200)-35	EHTPB-1000(200)	35	580	0.41
PU-1000(200)-45	EHTPB-1000(200)	45	880	0.45
PU-1000(200)-55	EHTPB-1000(200)	55	1310	0.27
PU-1000(200)-69	EHTPB-1000(200)	69	2380	0.36
PU-1650(210)-35	EHTPB-1650(210)	35	940	0.28
PU-2300(200)-35	EHTPB-2300(200)	35	1340	0.70
PU-4200(210)-35	EHTPB-1000(210)	35	2410	0.55

[a] The hard segment number average molecular weight was calculated by the method[32] of $M_{nH} = M_{ns}(100 - S_c)/S_c$, where M_{nH} is the hard segment number average molecular weight, M_{ns} is the soft segment number average molecular weight, and S_c is the soft segment content (wt %).

to a stirring MDI solution under dry nitrogen at 60−70 °C. After 1.5 h, a required amount of chain extender solution (5% w/v) was added dropwise within 30−35 min. Chain extension with the stoichiometric amount of butanediol required 12 h. The total amount of reactants in the mixed solution was around 10% (w/v). The solution was clear throughout the reaction. Following the reaction, the polyurethanes were precipitated from a large amount of water and dried at 50 °C in a vacuum. The polyurethanes' yield all exceeded 97%. Many polyurethanes had been synthesized; however, only a few were found useful for this present study. Table 2 lists the composition and properties of the polyurethanes under this study. Sample code is expressed as PU-*xxxx*(*yyy*)-*zz*, where *xxxx* denotes the EHTPB's number average molecular weight before epoxidation, *yyy* denotes the value of WPE in the soft segment, and *zz* denotes the hard segment content.

The polymer films were prepared by casting a solution of 10% polyurethane in DMAc on a Teflon mold, followed by drying at 50 °C for 3 days in vacuum. The films were stored in a desiccator under room temperature for at least 7 days before analysis. The films were transparent to visible light.

2. Characterization Method. Intrinsic viscosities of EHTPB-based PUs were determined by a Cannon-Fenske viscometer at 30 ± 0.05 °C in DMAc solution.

Synchrotron SAXS experiments were conducted on the State University of New York (SUNY) X3A2 beamline, National Synchrotron Light Source, Brookhaven National Laboratory (NSLS). A modified Kratky camera and a Braun position-sensitive detector were used at an X-ray wavelength of 0.154 nm. The distance from the sample to detector was 1290 mm. The beam size at the sample position was ~0.2 × 2 mm^2. Next, the synchrotron beam was focused into the beam stop which was ~40 mm in front of the Braum detector having a receiving window width of ~2 mm. Therefore, smearing effect on the SAXS patterns was negligible. Routine correction procedures, except for the absolute intensity calibration, were performed on SAXS data.

DSC measurements were performed using a Perkin-Elmer DSC7 with a liquid nitrogen cooler in a helium atmosphere. Cyclohexane and indium were used for two-point temperature calibration. Indium was used to calibrate heat capacity. The sample weight was roughly 10 mg. The cast samples were initially quenched from room temperature to −100 °C at a cooling rate of 320 °C/min and then scanned up at a rate of 20 °C/min for DSC measurement. The melt-quenched samples were initially heated to 230 °C (above the highest endothermic transition exhibited by the PUs) at a rate of 40 °C/min and held at that temperature for 5 min to enhance the segmental mixing. The sample was then quenched to −100 °C at a rate of 320 °C/min and then scanned up to 230 °C at a rate of 20 °C/min for DSC measurement. At least three samples were run for each glass transition behavior.

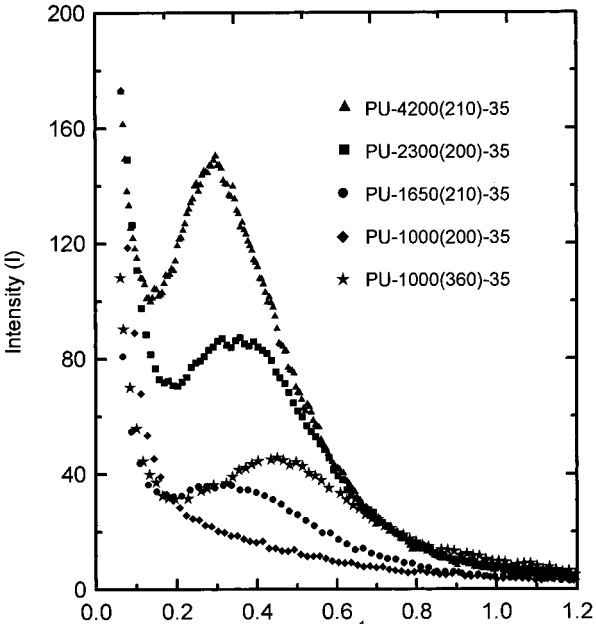

Figure 4. The SAXS patterns of PU-*xxxx*(200)-35 samples with 1000, 1650, 2300, and 4200 soft segment number average molecular weight, respectively. The SAXS pattern of PU-1000-(360)-35 sample is also included.

Results and Discussion

SAXS Analysis. Figure 4 shows the SAXS patterns of PU-*xxxx* (200~210)-35 samples with the soft segment molecular weight of 1000, 1650, 2300, and 4200, respectively. Except PU-1000(200)-35, all other samples show a scattering peak. Since scattering peak height is roughly proportional to the contrast between the phases, the scattering peak height increases with the increase in soft segment molecular weight, indicating the longer the soft segment length, the higher the degree of microphase separation. This is due to incompatibility between the two block increases as the length of either block increases. SAXS studies on the effect of epoxide concentration in the soft segment is also illustrated in Figure 4. The cast PU-1000(360)-35 sample has a lower epoxide concentration in the soft segment than that of PU-1000(200)-35. The SAXS shows a small scattering peak for PU-1000(360)-35. This indicates that the electron density variance in PU-1000(360)-35 is higher than that in PU-1000(200)-35. This higher electron density variance is due to a higher extent of microphase separation which leads to a greater contrast in electron densities.

On the basis of the above SAXS analyses, we understand that a homogeneous polyurethane sample may be obtained by using a EHTPB with the average molecular weight at 1000 and the WPE value at 200. Figure 5 shows the SAXS patterns of the cast PU-1000(200)-*zz* samples with 28%, 35%, 45%, and 55% hard segment

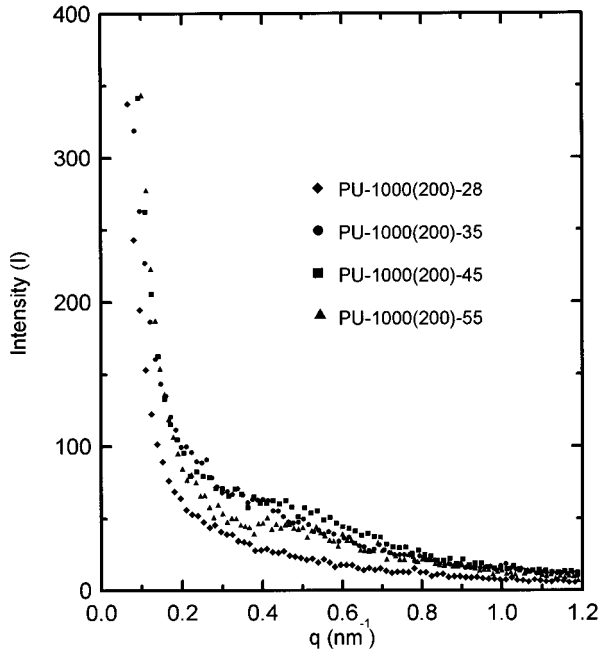

Figure 5. The SAXS patterns of PU-1000(200)-*zz* samples with 28%, 35%, 45%, and 55% hard segment content, respectively.

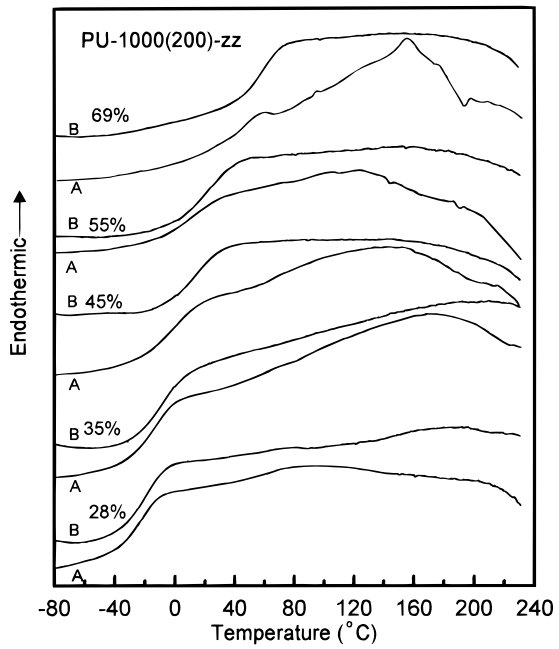

Figure 6. The DSC thermograms for PU-1000(200)-*zz* samples with 28%, 35%, 45%, 55%, and 69% hard segment contents, respectively. All A curves were measured for the samples cast from DMAc solution. All B curves were measured for the samples preheated at 230 °C for 5 min and followed by quenching at a rate of 320 °C per min to −100 °C.

contents, respectively. There are almost no scattering peaks as the hard segment content ranges from 28% to 55%. This indicates that all the PU-1000(200)-*zz* samples are nearly homogeneous.

DSC Analysis. The A curves in Figure 6 show the DSC thermograms of PU-1000(200)-*zz* samples with 28%, 35%, 45%, 55%, and 69% hard segment contents, respectively. However, there are some endothermic behaviors appearing above 60 °C, indicating phase separation is not quite complete. In light of these observations, we believe the DSC analysis for the determination of the microphase separation may be more sensitive than the SAXS analysis. On the other hand, all the glass transition temperatures of these polyurethanes are all much higher than the glass transition temperature of EHTPB polyol ($T_g = -65$ °C) for at least 40 °C. This indicates that the hard segments and the soft segments are highly mixed.

Table 3. Thermal Transition Behaviors of EHTPB-1000(200) Prepolymer and the Melt-Quenched PU-1000(200)-*zz* Polyurethane Samples

EHTPB sample	glass transition temperature, T_{g_m} (°C)	breadth at T_{g_m}, ΔB_m[a] (°C)	heat capacity, ΔC_{p_m} (J/g °C)	$\Delta C_{p_m}{}^S$ (J/g °C)[b]
EHTPB-1000(200)	(−65)[c]	(6)[c]	(0.57)[c]	(0.57)[c]
PU-1000(200)-28	−17	35	0.52	0.72
PU-1000(200)-35	−8	35	0.50	0.76
PU-1000(200)-45	15	36	0.48	0.87
PU-1000(200)-55	23	38	0.47	1.03
PU-1000(200)-69	57	34	0.43	1.39

[a] ΔB_m was measured from onset to end. [b] $\Delta C_{p_m}{}^S$ was defined as ΔC_{p_m}/per unit mass of the soft segment. [c] The glass transition behavior of EHTPB-1000(200) sample, show here for the comparison.

In order to enhance the compositional homogeneity, melt-quenched experiments were performed. PU-1000-(200)-*zz* samples were first brought to 230 °C, which exceeds the highest endothermic temperature, and held for 5 min to ensure the formation of a complete phase-mixed homogeneous state. If a homogeneous state was obtained at 230 °C and a quench rate was fast enough to freeze the morphology at 230 °C, the resultant frozen-in mixed phase may exhibit only a single glass transition behavior. The B curves in Figure 6 show the DSC thermograms of melt-quenched samples. All these curves give rise to only a single glass transition behavior, and all these curves are very level before and after the glass transitions. These phenomena clearly evidence that the melt-quenched samples have reached a completely homogeneous phase. Table 3 summarizes the glass transition behaviors of the melt-quenched samples, including the glass transition temperature, T_{g_m}, the breadth of T_{g_m}, ΔB_m, and the specific heat capacity at T_{g_m}, ΔC_{p_m}. Glossary of terms are listed in Table 4.

Generally speaking, a blend may exhibit a broader ΔB_m owing to the presence of some inhomogeneity in the mix. Because higher hard segment content is equivalent to higher hard segment molecular weight in the samples, these samples with increasing hard segment content may give rise to some inhomogeneity owing to the higher hard segment molecular weight. Thus, an increase in hard segment content may cause an increase in ΔB_m. However, as the hard segment content increases from 28% to 69%, ΔB_m's of the melt-quenched PU-1000(200)-*zz* samples remain roughly constant (as shown in Table 3). This result further suggests that the segmental mixing in the melt-quenched sample is very complete.

As has been generally mentioned in the literatures,[5,7,15,16,24] if the contribution from the heat capacity of the MDI−BD hard segment, while mixed with the soft segment, can be neglected, ΔC_{p_m} per gram of the soft segment ($\Delta C_{p_m}{}^S$ in Table 3) should be constant and roughly equal to EHTPBs specific heat capacity (0.57 J/g °C). However, $\Delta C_{p_m}{}^S$ significantly increases as the hard segment content increases. This phenomenon indicates that the hard segment heat capacity cannot be neglected. The hard segment does contribute significantly to the observed ΔC_p change of the melt-quenched samples.

Table 4. Glossary of Terms

T_{g_m}:	glass transition temperature of the polyurethanes in mixed homogeneous state
ΔB_m:	breadth of glass transition temperature of the polyurethanes in mixed homogeneous state
ΔC_{p_m}:	specific heat capacity of the polyurethanes in mixed homogeneous state
$\Delta C_{p_m}{}^S$:	specific heat capacity of the polyurethanes in mixed homogeneous state per unit mass of soft segment
$T_{g_{H^\circ}}$:	glass transition temperature of the pure hard segment
$T_{g_{S^\circ}}$:	glass transition temperature of the pure soft segment
$T_{g_{HP}}$:	glass transition temperature of the hard phase
$T_{g_{SP}}$:	glass transition temperature of the soft phase
$\Delta C_{p_{SP}}$:	change in specific heat capacity of the soft phase in the copolymer per unit mass of copolymer
$\Delta C_{p_{H^\circ}}$:	change in specific heat capacity of the ideally microphase-separated hard phase per unit mass of pure component material
$\Delta C_{p_{S^\circ}}$:	change in specific heat capacity of the ideally microphase-separated soft phase per unit mass of pure component material
W_S:	weight fraction of the soft segment in the copolymer
W_H:	weight fraction of the hard segment in the copolymer
W_{SP}:	weight fraction of the soft phase
W_{HP}:	weight fraction of the hard phase
W_{SS}:	weight fraction of the soft segment in the soft phase
W_{HS}:	weight fraction of the hard segment in the soft phase
W_{HH}:	weight fraction of the hard segment in the hard phase
W_{SH}:	weight fraction of the soft segment in the hard phase

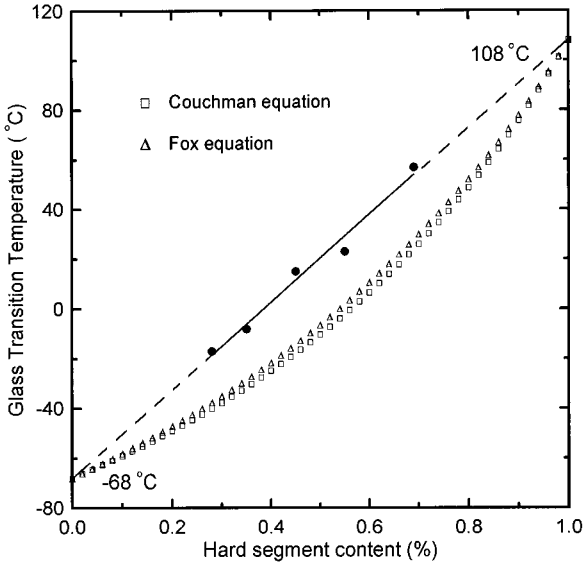

Figure 7. Plot of the glass transition temperatures for the melt-quenched PU-1000(200)-*zz* samples.

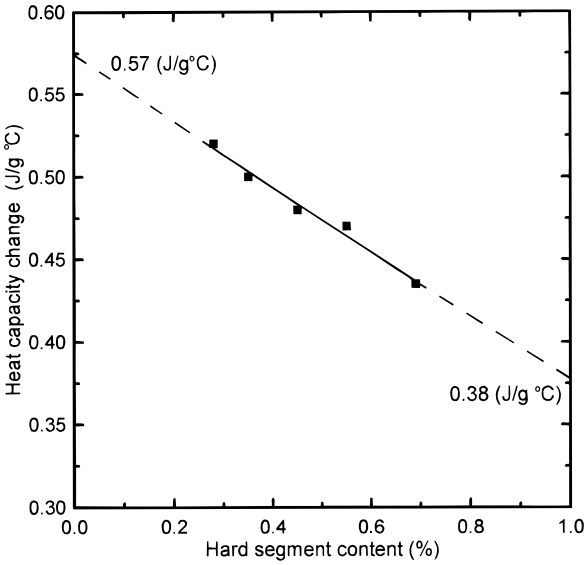

Figure 8. Plot of the observed heat capacity change for the melt-quenched PU-1000(200)-*zz* samples.

Figures 7 and 8 show the variations of the observed T_{g_m} and ΔC_{p_m}, respectively, with the hard segment content in the PU-1000(200)-*zz* samples. T_{g_m} increases linearly with the increase in the hard segment content. ΔC_{p_m} decreases linearly with the increase of the hard segment content. When one extrapolates to 100% hard segment content, the resulting pure hard segment T_g and ΔC_p are 108 °C and 0.38 J/g °C, respectively. These values are equal to the reported[24] T_g (107 °C) and ΔC_p (0.39 J/g °C) of a high molecular weight MDI−BD polymer. On the other hand, the extrapolation of T_{g_m} and ΔC_{p_m} to 0% hard segment gives rise to $T_g = -68$ °C and $\Delta C_p = 0.57$ J/g °C; these values are also equivalent to EHTPB prepolymer's T_g (−65 °C) and ΔC_p (0.57 J/g °C), respectively. Among these pure component properties, $\Delta C_{p_{H^\circ}}$ of 0.38 J/g °C deserve much attention, since a reliable value of $\Delta C_{p_H}{}^\circ$ has never been experimentally obtained before. On the other hand, the extrapolated results in Figures 7 and 8 also indicate that previous assumptions[5,7,24] on the methods to define the T_g of the pure hard segment and the T_g and ΔC_p of the pure soft segment are correct. On the basis of the values of these pure component properties, T_{g_m} and ΔC_{p_m} can be obtained by the following equations:

$$T_{g_m} = W_S T_{g_{S^\circ}} + (1 - W_S) T_{g_{H^\circ}} \quad (1)$$

$$\Delta C_{p_m} = W_S \Delta C_{p_{S^\circ}} + (1 - W_S) \Delta C_{p_{H^\circ}} \quad (2)$$

where W_S represents the weight fraction of the soft segment in the copolymer.

In segment polyurethanes of constant soft segment molecular weight, the increase in the hard segment content causes an increase in the hard segment molecular weight (shown in Table 2). Thus, the linear relationships in Figures 7 and 8 may indicate that the contributions of the hard segments to T_{g_m} and ΔC_{p_m} are independent of the hard segment length. Furthermore, the linear relationship may also indicate that chemical functions between blocks do not act in the same fashion as end groups to a sequence length dependence. At least, they appear to be so.

Both eqs 1 and 2 correspond to the generally accepted principle that the observed change in a thermal property of a single-phase two-component system is the linear weighted addition of the two individual component changes in that property. However, eq 1 is not well-adopted in the literatures. A number of equations that express the relationship have appeared,[10−12,18,25−27] both of thermodynamic and empirical origin. The most general form from thermodynamic origin is that of the Couchman equation,[10−12]

$$\ln T_{g_m} = (W_S \Delta C_{p_{S^\circ}} \ln T_{g_{S^\circ}} + W_H \Delta C_{p_{H^\circ}} \ln T_{g_{H^\circ}})/(W_S \Delta C_{p_{S^\circ}} + W_H \Delta C_{p_{H^\circ}}) \quad (3)$$

On the other hand, the most general form from empirical origin is that of the Fox equation,

$$1/T_{g_m} = W_S/T_{g_{S^\circ}} + W_H/T_{g_{H^\circ}} \quad (4)$$

where W_S and W_H are the weight fractions of the soft segment and the hard segment, respectively, in the copolymer. Figure 7 also plots eqs 3 and 4 on the basis of the T_g and ΔC_p of both the pure hard segment and the pure soft segment obtained in this study. Apparently, both these equations cannot model the observed T_g behavior in our current polyurethane system.

Although the most rigorous Couchman's equation has successfully applied to many blends and has received many attentions in the sense that various other equations can be derived from it by making simplified assumptions, there are a number of systems in which deviations from Couchman's equation are significant.[28−30] Some of the largest differences have been observed in those systems where hydrogen bond interactions between the different components are strong.[28−30] It is possible that the formation of hydrogen bonds between MDI−BD hard segments and the epoxide group on the EHTPB soft segment would similarly contribute to some deviation from Couchman's equation. The relation of linear weighted combinations shown in eq 1 shall not be too surprising. Furthermore, commercial polyurethanes are generally based on polyester polyol or polyether polyol as the soft segment. There also exists a strong hydrogen bond interaction between the MDI−BD hard segment and the carbonyl or ether oxygen atom on the soft segment. The situation is similar to that of our EHTPB-based polyurethanes. With regard to these comparisons, eqs 1 and 2 from this study may be the most adequate method for calculating commercial polyurethanes' microphase composition.

Equations 1 and 2, while applied to a fully amorphous soft phase in a partially phase-separate polyurethane system, would take the forms of

$$T_{g_{SP}} = W_{SS} T_{g_{S^\circ}} + (1 - W_{SS}) T_{g_{H^\circ}} \quad (5)$$

$$\Delta C_{p_{SP}}/W_{SP} = \Delta C_{p_{S^\circ}} W_{SS} + \Delta C_{p_{H^\circ}}(1 - W_{SS}) \quad (6)$$

where $T_{g_{SP}}$ is the glass transition temperature of the soft phase, $\Delta C_{p_{SP}}$ is the observed change in specific heat capacity of the soft phase in the copolymer per unit mass of copolymer, W_{SP} is the weight fraction of the soft phase, and W_{SS} and W_{HS} are weight fractions of the soft segment in the soft phase and the hard segment in the soft phase, respectively. With W_{SS} obtained from eq 5, eq 6 is important in accessing the weight fraction of the soft phase, W_{SP}. However, the use of eq 6 for a MDI−BD-based polyurethane is generally hampered by the lack of the hard segment heat capacity, $\Delta C_{p_{H^\circ}}$. $\Delta C_{p_{H^\circ}}$ of 0.38 J/g °C obtained from this study is important in this respect. Furthermore, with the known value of the soft phase weight fraction, a level rule can be used to calculate the weight fraction of hard segments in a hard-segment-rich microdomain, W_{HH}:

$$W_{HH} = (W_H - W_{SP} W_{HS})/(1 - W_{SP}) \quad (7)$$

From the above processes, eqs 5−7 provide complete information for calculating the microphase composition and the degree of phase separation. However, our separate study on a series of complete phase-separated polyurethanes has recently found that the ΔC_p of a phase-separated microdomain is highly dependent on the domain morphology and the segment molecular weight. While we have just found the long-term confusing value of pure hard segment ΔC_p for use in eq 6, ironically, we simultaneously indicate that the ΔC_p of a phase-separated domain at around 10 nm is inadequate for quantitative use. Unfortunately, microdomains of commercial polyurethanes generally fall in this range. A paper for this detail has been submitted for publication.

Conclusion

We developed a new type of soft segment prepolymer, epoxidized hydroxyl-terminated *cis*-polybutadiene (EHTPB) to synthesize a series of segment polyurethanes which are based on MDI−BD as the hard segment. Increasing the EHTPB epoxide content and/or decreasing the EHTPB molecular weight will finally lead to a completely phase-mixed polyurethane material. A single glass transition temperature was found for each homogeneous polyurethane. Attempts were made to find the long-term confusing T_g and ΔC_p of the pure MDI−BD hard segment in polyurethane materials. By extrapolating the observed T_g and ΔC_p for the homogeneous polyurethanes to 100% hard segment content, the pure hard segment T_g and ΔC_p thus obtained are 108 °C and 0.38 J/g °C, respectively. These values are just equal to the reported T_g and ΔC_p of a high molecular weight MDI−BD homopolymer. In addition, extrapolating the values of the observed T_g and ΔC_p for the homogeneous polyurethanes to 0% hard segment, we obtained that the pure soft segment T_g and ΔC_p are −68 °C and 0.57 J/g °C, respectively. These values are also equal to the T_g and ΔC_p of the soft segment prepolymer, EHTPB, indicating that the previous assumption[5,24] to define the pure soft segment T_g and ΔC_p is correct. Furthermore, both the observed T_g and ΔC_p of the homogeneous polyurethanes are found to be results of a linear weighted combination of the pure constituent materials and to be independent of the segment molecular weights. This simple relationship and values of the pure hard segment T_g and ΔC_p obtained herein provide useful information to calculate the microphase composition and the degree of phase separation in segment polyurethanes, providing that the morphology of the microdomains would not seriously affect the specific heat capacity for each microdomain. *Ironically, while we have just found a reliable pure hard segment ΔC_p value, which makes the calculation of the weight fraction of the soft phase possible, our other study evidences that any "quantitative" use of the heat capacity change in a polyurethane microdomain is not correct, since heat capacity change in a microdomain of around 10 nm can be greatly affected by the microdomain morphology and the segment molecular weight.* These later phenomena are discussed in a separate paper.

Acknowledgment. The authors are grateful to the National Science Council of the Republic of China for the financial support. The authors are also grateful to both professor Benjamin Chu and Mr. Feng-Ji Yeh (Department of Chemistry, The State University of New York, Stony Brook, New York) for kindly assisting us in acquiring the SAXS data.

References and Notes

(1) Van Bogart, J. W. C.; Gibson, P. E.; Cooper, S. L. *J. Polym. Sci., Polym. Phys. Ed.* **1983**, *21*, 65.
(2) Brunette, C. M.; Hsu, S. L.; Macknight, W. J.; Schneider, Nl S. *Polym. Eng. Sci.* **1981**, *21*, 163.
(3) Brunette, C. M.; Hsu, S. L.; Macknight, W. J.; Schneider, N. S. *Polym. Eng. Sci.* **1981**, *21*, 668.
(4) Hong, J. L.; Lillya, C. P.; Chien, J. C. W. *Polymer* **1992**, *33*, 4347.
(5) Camberlin, Y.; Pascault, J. P. *J. Polym. Sci., Polym. Chem. Ed.* **1983**, *21*, 415.
(6) Petrovic', Z. S.; Javni, I. *J. Polym. Sci., Polym. Phys. Ed.* **1989**, *27*, 545.
(7) Leung, L. M.; Koberstein, J. T. *Macromolecules* **1986**, *19*, 706.
(8) Tao, H. J.; Fan, C. F.; Macknight, W. J.; Hsu, S. L. *Macromolecules* **1994**, *27*, 1720.
(9) Wagener, K. B.; Matayabas, J. C., Jr. *Macromolecules* **1991**, *24*, 618.
(10) Couchman, P. R.; Karasz, F. E. *Macromolecules* **1978**, *11*, 117.
(11) Couchman, P. R. *Macromolecules* **1978**, *11*, 1156.
(12) Couchman, P. R. *Polym. Eng. Sci.* **1984**, *24*, 135.
(13) Speckhard, T. A.; Gibson, P. E.; Cooper, S. L.; Chang, V. S. C.; Kennedy, J. P. *Polymer* **1985**, *26*, 55.
(14) Phillips, R. A.; Stevenson, J. C.; Nagarajan, M. R.; Cooper, S. L. *J. Macromol. Sci., Phys.* **1988**, *B27*, 245.
(15) Koberstein, J. T.; Leung, L. M. *Macromolecules* **1992**, *25*, 6025.
(16) Cuve', L.; Pascault, J. P.; Boiteux, G. *Polymer* **1992**, *33*, 3957.
(17) Macknight, W. J.; Yang, M.; Kajiyama, T. *Polym. Prepr.* **1968**, *9* (1), 860.
(18) Wood, L. A. *J. Polym. Sci.* **1958**, *28*, 319.
(19) Koberstein, J. T.; Galambos, A. F.; Leung, L. M. *Macromolecules* **1992**, *25*, 6195.
(20) Hu, W.; Koberstein, J. T. *J. Polym. Sci., Polym. Phys. Ed.* **1994**, *32*, 437.
(21) Boyer, R. F. *J. Polym. Sci., Polym. Symp.* **1975**, *50*, 189.
(22) Chen, T. K.; Hwung, C. T. *Proc. 10th, ROC Polym. Symp.* **1987**, P790.
(23) Chen, T. K.; Chui, J. Y. *Proc. 10th, ROC Polym. Symp.* **1995**, P495.
(24) Cuve', L.; Pascault, J. P.; Boiteux, G.; Seytre, G. *Polymer* **1991**, *32*, 343.
(25) Fox, T. G. *Bull. Am. Phys. Soc.* **1956**, *1*, 123.
(26) Gordon, M.; Taylor, J. S. *J. Appl. Chem.* **1952**, *2*, 495.
(27) Kwei, T. K. *J. Polym. Sci., Polym. Lett. Ed.* **1984**, *22*, 307.
(28) Kwei, T. K.; Charton, M.; Pearce, E. M.; Pennacchia, J. R. *Macromolecules* **1987**, *20*, 1174.
(29) Lee, J. Y.; Coleman, M. M.; Moskala, E. J.; Painter, P. C. *Appl. Apectrosc.* **1986**, *40*, 991.
(30) Goh, S. H.; Siow, J. S. *Polym. Bull.* **1987**, *17*, 453.
(31) Ray, R. R. *Anal. Chem.* **1964**, *36* (3), P6617.
(32) Petrovic', Z. S.; Budinski-Simedic', J. *Rubber Chem. Technol.* **1985**, *58*, 685.

MA9618639